Conformational Changes and Orientation of *Humicola lanuginosa* Lipase on a Solid Hydrophobic Surface: An in Situ Interface Fourier Transform Infrared-Attenuated Total Reflection Study

Sylvie Noinville,* Madeleine Revault,* Marie-Hélène Baron,* Ali Tiss,† Stéphane Yapoudjian,† Margarita Ivanova,† and Robert Verger†

*Laboratoire de Dynamique, Interactions et Réactivité, Centre National de la Recherche Scientifique, Université Paris 6, 94320 Thiais, France; and †Laboratoire de Lipolyse Enzymatique, Centre National de la Recherche Scientifique-IFR1, 13402 Marseille, France

ABSTRACT This study was done to better understand how lipases are activated at an interface. We investigated the conformational and solvation changes occurring during the adsorption of *Humicola lanuginosa* lipase (HLL) onto a hydrophobic surface using Fourier transform infrared-attenuated total reflection spectroscopy. The hydrophobic surfaces were obtained by coating silicon attenuated total reflection crystal with octadecyltrichlorosilane. Analysis of vibrational spectra was used to compare the conformation of HLL adsorbed at the aqueous-solid interface with its conformation in solution. X-ray crystallography has shown that HLL exists in two conformations, the closed and open forms. The conformational changes in HLL caused by adsorption onto the surface were compared with those occurring in three reference proteins, bovine serum albumin, lysozyme, and α-chymotrypsin. Adsorbed protein layers were prepared using proteins solutions of 0.005 to 0.5 mg/mL. The adsorptions of bovine serum albumin, lysozyme, and α-chymotrypsin to the hydrophobic support were accompanied by large unfoldings of ordered structures. In contrast, HLL underwent no secondary structure changes at first stage of adsorption, but there was a slight folding of β-structures as the lipase monolayer became complete. Solvation studies using deuterated buffer showed an unusual hydrogen/deuterium exchange of the peptide CONH groups of the adsorbed HLL molecules. This exchange is consistent with the lipase being in the native open conformation at the water/hydrophobic interface.

INTRODUCTION

Lipases (triacylglycerol hydrolases, EC 3.1.1.3) are a special class of esterases that hydrolyze triacylglycerols at lipid/water interfaces. They also have interesting industrial applications (Bornscheuerand and Kazlauskas, 1999; Alberghina, 2000; Schmid and Verger, 1998). In contrast to most esterases, the catalytic activity of lipases increases dramatically when a partially water-soluble substrate becomes insoluble (Sarda and Desnuelle, 1958; Ferrato et al., 1997). This phenomenon of interface activation was originally detected in studies on porcine pancreatic lipase and was attributed to a conformational change (Desnuelle et al., 1960). The three-dimensional crystal structures of several lipases have been determined (Brady et al., 1990; Winkler et al., 1990; Derewenda et al., 1994a; Roussel et al., 1999). All the lipases have an α/β-hydrolase fold structure (Ollis et al., 1992) with a catalytic triad similar to the one found in serine proteases. The active site is generally buried under a lid or flap, containing an amphiphilic α-helix, making the active site inaccessible to the substrate in the so-called closed conformation. The three-dimensional structure of lipases complexed with inhibitors or co-crystallized in the presence of micelles shows that the lid is rearranged to make the active site accessible to substrates (Brzozowski et al., 1991; Tilbeurgh et al., 1993; Lawson et al., 1994). Opening the lid exposes a large hydrophobic surface, whereas the previously exposed hydrophilic domain becomes buried inside the protein (Grochulski et al., 1993; Derewenda et al., 1994a; Tilbeurgh et al., 1993).

However, no direct structural data have yet been produced to demonstrate that the interfacial activation of lipases, based on enzyme kinetics, is directly linked to a conformational change caused by adsorption. Lipases have been widely investigated, and their activity and adsorption properties have been determined using monomolecular lipid films at an air/water interface (Ransac et al., 1997; Peters et al., 1998; Momsen and Brockman, 1997). However, there have been few detailed studies on the adsorption of lipases to solid surfaces (Wannerberger and Arnebrant, 1996; Duinhoven et al., 1995). We have therefore used surface infrared spectroscopy at an aqueous-solid interface to investigate the conformation of *Humicola lanuginosa* lipase (HLL) at an interface.

The most important features of protein adsorption to surfaces are the amounts of adsorbed proteins, the kinetics of adsorption, and the putative structural changes (Malmsten, 1998). Infrared spectroscopy is well suited for the spectral analysis of proteins and peptides in both the adsorbed and soluble states. Previous studies have reported a correlation between infrared spectra and the secondary structure of a protein (Goormaghtigh et al., 1990; Fu et al., 1993). Infrared spectroscopy, especially the use of attenuated total reflection (ATR) techniques, allows us to describe

Submitted September 28, 2001, and accepted for publication January 18, 2002.

Address reprint requests to Dr. S. Noinville, Laboratoire de Dynamique, Interactions et Réactivité, Centre National de la Recherche Scientifique, 2 rue Henri Dunant, 94320 Thiais, France. Tel.: 00-33-149-781-292; Fax: 00-33-149-781-118; E-mail: sylvie.noinville@glvt-cnrs.fr.

© 2002 by the Biophysical Society

0006-3495/02/05/2709/11 $2.00

the structure of an adsorbed protein in an aqueous environment (Ball and Jones, 1995; Oberg and Fink, 1998; Chittur, 1998). Hydrogen isotope exchange techniques are also very powerful for analyzing protein structure and dynamics in biological systems (Gregory and Lumry, 1985). The decrease in the infrared amide II band is proportional to the number of hydrogen in amide CONH that have been replaced by deuterium. Thus, the H/^{2}H exchange measurement provides useful information about the protein solvation and/or changes in the tertiary structure.

We have compared the adsorption of a lipase and such well-characterized proteins as bovine serum albumin (BSA), lysozyme, and α-chymotrypsin with a hydrophobic support. The present paper describes the adsorption kinetics as well as the H/^{2}H exchange for these globular proteins, having different binding and/or catalytic properties. BSA has binding properties, whereas lysozyme and α-chymotrypsin have hydrolytic activities in solution. In contrast, the lipolytic activity of HLL is monitored by adsorption. The main interactions involved in the adsorption of proteins are hydrophobic and electrostatic interactions and hydrogen bonding (Andrade et al., 1992; Kondo et al., 1992). Structural stability in solution as well as the distributions of polar and hydrophobic amino acid residues at the external shell of a protein are some of the many parameters influencing adsorption (Zoungrana et al., 1997; Norde, 2000). We have used BSA as an example of a protein with low structural stability in solution and lysozyme and α-chymotrypsin as more robust water-soluble proteins, more like HLL (Haynes and Norde, 1995). The hydrophobic residues at the external surface of lysozyme, α-chymotrypsin, and BSA are randomly distributed unlike those of HLL. Thus, the adsorption and affinity of each protein studied should be quite different when they are adsorbed on a hydrophobic surface. The secondary structure, solvation, and protonation states of these four proteins were determined when they were adsorbed and in solution.

MATERIALS AND METHODS

Materials

Highly purified recombinant lipase from HLL was kindly provided by Dr. Sham Patkar and Dr. Allan Svendsen of Novo-Nordisk (Bagsvaerd, Denmark). HLL contains 269 amino acids with 179 H bonds (Derewenda et al., 1994c). Its isoelectric point is 4.4 (Martinelle et al., 1995). HLL solutions were dialyzed three times against sodium phosphate buffer (55 mM Na_2HPO_4, pH 7.5) and lyophilized before use.

BSA (A-7638), α-chymotrypsin (C-4129), and lysozyme (L-6876) were obtained from Sigma (St Louis, MO) and used without further purification. Their isoelectric points are: 4.8 for BSA (Quiquampoix and Ratcliffe, 1992), 8.6 for α-chymotrypsin (Baron et al., 1999), and 11 for lysozyme (Imoto et al., 1972).

Solutions of proteins were prepared by dissolving the lyophilized powder in deuterated phosphate buffer (55 mM $Na_2{}^2HPO_4$), adjusted to a p^{2}H of 7.5 with ^{2}HCl. The HLL concentration was 0.005 to 0.5 mg/mL for ATR experiments and 5 mg/mL for Fourier transform infrared (FTIR) transmission experiments. For the three other proteins (BSA, lysozyme, and α-chymotrypsin), a concentration of 0.01 mg/mL was used for ATR experiments and 4 mg/mL for FTIR transmission experiments.

Octadecyltrichlorosilane (OTS) (Roth, France) was used without further purification. The carbon tetrachloride (Prolabo, France) used for silanization was distilled before use. Hexadecane (SDS, France) was percolated through an Al_2O_3 column to remove trace of hydrophilic contaminants.

Treatment of the silicon ATR crystal surface

The ATR crystal was monocristalline silicon Si(100). The thin native oxide layer on the silicon ATR crystal enables alkyltrichlorosilanes to be grafted to it to obtain highly hydrophobic surfaces in a very reproducible way. The hydrophobic silanized surfaces were prepared by immersing the cleaned ATR crystal in a solution of OTS (Netzer and Sagiv, 1983). The concentration of OTS was 0.05 M in carbon tetrachloride/hexadecane (30:70, v/v). The area (22 Å^2) occupied by an OTS molecule was calculated from the area of the CH_2 stretching bands using the Sperline equation (see Surface density measurements), which is consistent with a closely packed quasi-crystalline layer (Wasserman et al., 1989).

FTIR experiments

FTIR spectra of proteins in solid state were recorded using a Bruker IR scope II microscope interfaced to a Bruker Equinox spectrometer. The lyophilized protein powder was spread over a KBr window so that the thin protein sample transmitted IR energy.

The recording of H/^{2}H exchange kinetics by FTIR is not a standard method. The experimental procedure we used was as follows. The beginning of the adsorption and/or H/^{2}H exchange kinetics was set at the dissolution of the lyophilized protein in the deuterated phosphate buffer for both transmission and ATR experiments, unless otherwise specified.

For transmission measurements, the protein solution is placed in a CaF_2 cell with a 50-μm spacer. Spectra were recorded from 8 min to 2 h at various times. The minimal time required to record the first infrared spectrum was 8 min to ensure the removal of water vapor, which absorbs in the spectral region of interest. The spectrum of the protein itself was the difference that of the protein solution and that of the buffer (Fig. 1).

The internal reflection element used was a 45° cut silicon crystal mounted in an ATR liquid cell (Ball and Jones, 1995). The ATR crystal, whose dimensions were 40 × 15 × 0.4 mm, provided 75 internal reflections at the liquid/crystal interface. The ATR liquid cell was filled with the deuterated buffer and a reference infrared spectrum was recorded for 8 min to 2 h. The cell was then emptied and filled with the protein solution; interferograms were recorded as for the reference spectrum, and transformed to an absorption spectrum of the adsorbed protein. Each spectrum was an average of 300 scans.

Transmission and FTIR-ATR spectra were recorded on a Perkin-Elmer 1720 and on a Nicolet 850 FTIR-spectrometer, respectively. The sample compartment of each spectrometer was continuously purged with dried air. All infrared spectra were recorded with Boxcar apodization and a resolution of 4 cm^{-1}.

Surface density measurements

The ATR method was used to follow the adsorption of the protein onto the treated silicon ATR crystal. The amount of protein adsorbed on the solid support was estimated from the following adsorption density equation (Sperline et al., 1987):

$$\Gamma = \frac{\frac{A}{N} - \varepsilon C_b d_e}{2000\varepsilon \frac{d_e}{d_p}} \quad (1)$$

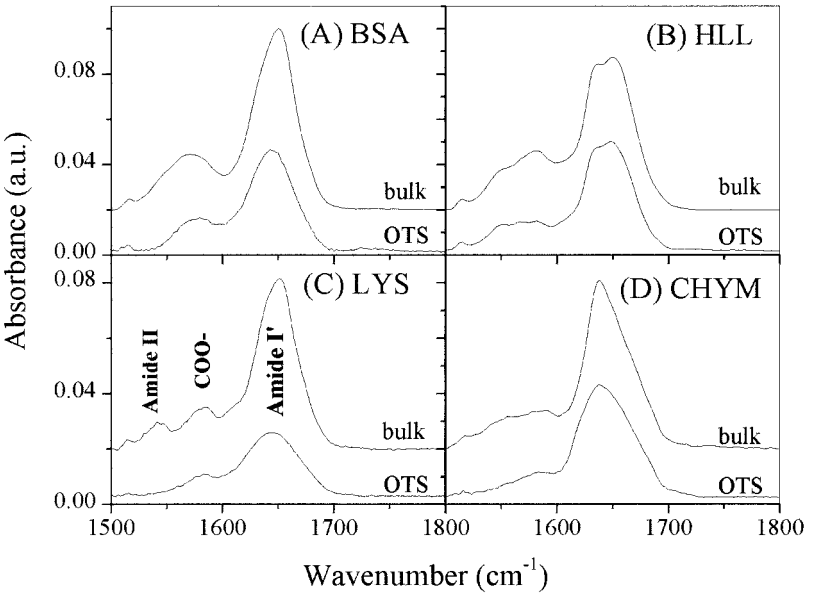

FIGURE 1 Infrared transmission spectra of the proteins recorded after 2 h in deuterated phosphate buffer (0.055 M $Na_2{}^2HPO_4$) (bulk) and ATR spectra of the adsorbed proteins recorded after 2 h at the ^2H_2O/hydrophobic interface (OTS) for BSA (*A*), HLL (*B*), lysozyme (*C*), and α-chymotrypsin (*D*) at p^{2}H 7.5.

in which A was the integrated area of the amide I band (1600–1700 cm^{-1}), N was the number of internal reflections, C_b was the bulk protein concentration, and ϵ was the molar absorptivity determined from the transmittance spectrum. The penetration depth (d_p) and the effective thickness (d_e) were calculated from the equations given by Harrick (1967). The thickness of the OTS monolayer was determined by ellipsometry and did not exceed 3 nm. Using a d_p value of ~500 nm at 1650 cm^{-1}, the effect of the coated OTS on the attenuation of the evanescent wave at the buffer/silicon interface, with a refractive index of 1.3 (buffer) and 3.4 (silicon), was neglected. We assumed that the buffer refractive index was not significantly changed by the dilute concentrations of proteins used, so that the protein surface density (Γ) could be determined on line during adsorption. The amide I′ band was used to determine Γ, as the amide II region varies over time because of the slow NH/N^{2}H exchange.

The ATR measurements should be able to detect the irreversibly and reversibly adsorbed proteins as well as the protein in solution in the bulk subphase. However, the contribution to the overall spectrum of the protein present in solution is negligible compared with that of the adsorbed fraction for bulk protein concentrations lower than 1 mg/mL. Furthermore, the amount of reversibly adsorbed protein was negligible under the above experimental conditions, since replacing the protein solution with pure buffer did not decrease significantly the area under the amide I′ band (data not shown).

Spectral analysis

Fig. 1 shows the FTIR absorption spectra of the different proteins in solution and in the adsorbed state in the 1500 to 1800 cm^{-1} region. This spectral region covers three major groups of infrared absorption bands. One is the amide II band, corresponding to the peptide NH bending vibration modes (1530–1550 cm^{-1}). The second is the COO^- antisymmetric stretching bands due to the Asp and Glu carboxylate groups (1565–1585 cm^{-1}). The third is the broad amide I′ band corresponding to the peptide carbonyl stretching modes ν(CO) (1610–1700 cm^{-1}).

Second derivative analyses of the 1500 to 1800 cm^{-1} region gave 17 to 18 overlapping component bands, including amide II, carboxylate, and aromatic side-chains and amide I′ bands. The minima of the derivative spectrum for a given protein were at similar wave numbers for the ATR-FTIR and transmission spectra. Curve fitting was then performed using the Origin50 program by setting the number of component bands found by second-derivative analysis at fixed wave numbers with fixed bandwidth (12 cm^{-1}) and a PSVoigt profile (0.75 Gaussian/0.25 Lorentzian). The best-average fit gave the intensity of each component band for each spectrum.

The amide I′ absorption band in the 1610 to 1700 cm^{-1} range has eight component bands for HLL. The assignments of the component bands for HLL are shown in Table 1 and are deduced from the literature on spectrum-

TABLE 1 Component bands positions ν (cm^{-1}) fixed in curve-fitted spectra and attribution of the amide I′ components in deuterated solution

BSA ν (cm^{-1})	HLL ν (cm^{-1})	Lysozyme ν (cm^{-1})	α-Chymotrypsin ν (cm^{-1})	Assignments to ν(CO) peptide groups
1681	1692+1678	1689	1681+1691	"Free" CO in hydrophobic environment*
1671	1668	1670	1670	"Free" CO in polar environment*
1660 + 1651	1659+1648	1652	1651+1660	H-bonded CO in α-helices[†]
1640	1640	1641	1644	Hydrated CO[‡]
1630	1632	1630	1630+1638	H-bonded CO in bent, extended strands or β-sheets[†]
1612	1618	1610	1618	Intermolecular H-bonded CO in self-association[‡]

*See details in spectral analysis.
[†]Byler and Suzy (1986), Goormaghtigh et al. (1994) and references herein.
[‡]Wantyghem et al. (1990).

TABLE 2 Comparison of secondary structures resulting from our spectral analysis in deuterated solution (sol) and adsorbed at aqueous/solid interface (ads) at a bulk concentration of 0.01 mg/mL and p^{2}H 7.5

Secondary structure (in %)*	BSA			HLL					Lysozyme			α-Chymotrypsin		
		Ads			Ads					Ads			Ads	
	Sol†	10 min	2 h‡	Sol	10 min	20 min	2 h	19 h‡	Sol	10 min	2 h‡	Sol	10 min	4 h‡
Hydrophobic (random)	2	1	0	8	8	8	8	8	2	4	4	8	8	8
Polar (random)	10	13	14	10	11	11	11	12	16	17	16	12	12	10
Hydrated (random)	13	20	21	7	6	5	4	3	27	24	22	5	9	11
α-Helix	50	38	37	43	44	44	45	45	34	24	22	28	27	26
Bent, strand or sheet	23	23	22	27	28	29	30	32	11	16	19	40	32	31
Self-associated (random)	2	5	6	5	4	3	3	2	10	15	17	7	10	14

*The given values are the mean value of three experiments, standard deviations are ±1% of the overall peptide backbone.
†Values for each protein in solution are recorded at 2 h.
‡Corresponds to the maximum amount of protein adsorbed on OTS surface at the given bulk concentration.

structure correlations in ^2H_2O (Byler and Susi, 1986; Goormaghtigh et al., 1994). The β-sheets or β-strands generate two split contributions, a weak one in the 1670- to 1690-cm^{-1} region and an intense one near 1630 cm^{-1} (Surewicz and Mantsch, 1988). The band in the 1630- to 1638-cm^{-1} region could also be overlapped by the β-turns structures. Many authors indicate another contribution of the β-turns in the 1675- to 1685-cm^{-1} region (Krimm and Bandekar, 1986). As described previously (Wantyghem et al., 1990), the component bands around 1670 cm^{-1} and 1680 cm^{-1} may be assigned to the stretching of not-hydrogen bonded peptide carbonyls in polar (1670 cm^{-1}) and hydrophobic (1680 cm^{-1}) environments. Both the β-turns and the peripheral domains of β-sheets contain not-hydrogen bonded peptide carbonyls (Krimm and Bandekar, 1986), so that the IR bands at 1670 and 1680 cm^{-1} could include contributions from peptide carbonyls in β-structures or from random domains. The molar absorptivity is also larger for peptide carbonyls involved in β-strands and α-helices than for those in β-turns (de Jongh et al., 1996). If we assume that effects of vibrational coupling are weaker in globular proteins than in homopolypeptides, then we can ignore the weak overlapping contributions of β-structures to the high-frequency amide I′ region in our spectral analysis.

Table 1 also shows the positions and assignments of the component bands for the other proteins. The identified amide I′ component bands have been previously reported for BSA (Servagent-Noinville et al., 2000), α-chymotrypsin (Baron et al., 1999; Swedberg et al., 1990), and lysozyme (Prestrelski et al., 1991). Each amide I′ component band was correlated with the amount of peptide units involved in specific ordered structures (helix or strands), or in solvated or hydrophobic random coil domains of the protein. The ratio of the area under each component band to the area under the overall amide I′ band gives the fractions of the corresponding structures as a percentage of the overall polypeptide backbone.

Two IR component bands in the 1530 to 1550 cm^{-1} region were attributed to the amide II absorption band. The NH content of 100% corresponded to the amide II/amide I′ area ratio measured for the fully CONH proteins in solid state, which was 0.5 for BSA and lysozyme and 0.4 for HLL and α-chymotrypsin. This ratio revealed the different molar absorptivity coefficients for the amide I and amide II vibrational modes. During our experiments in bulk as well as at the water/OTS interface, the final peptide NH content, expressed in percentages, is obtained from the ratio of the area of the amide II bands over the area of the overall amide I′ band measured for the proteins in contact with ^2H_2O and referred to the amide II/amide I′ area ratio measured for the fully CONH proteins in solid state. A decrease in the number of NH peptide bonds (%) corresponded to an increase in the NH/N^{2}H exchange, meaning that ^2H_2O had solvated some new peptide bonds (CONH) inside the protein backbone (Pantazaki et al., 1998; Baron et al., 1999).

The infrared absorption bands in the 1565- to 1585-cm^{-1} range were assigned to the asymmetric stretching modes of COO^- for the deprotonated Asp and Glu side chains (Chirgadze et al., 1975). The Asp and Glu side-chain residues of all proteins were fully deprotonated in solution at p^{2}H 7.5. The ratio between the area under COO^- component bands and the area under the overall amide I′ band obtained from the spectra of proteins in solution corresponded to the reference value of 100% of COO^-. The COO^- content, expressed in percentages, was calculated from the COO^-/amide I′ area ratio obtained for the adsorbed state referred to the solution ratio.

Experiments were carried out three times for each bulk concentration. The relative integrated absorbance of the amide I′ component bands were determined within standard deviations of ±1% of the overall peptide backbone. The standard deviations for the NH and COO^- contents were within ±2% and ±5%, respectively, when the temperature was carefully controlled.

RESULTS AND DISCUSSION

Fig. 1 shows the spectra of HLL and the three other proteins (BSA, lysozyme, and α-chymotrypsin) adsorbed onto the hydrophobic surface and in solution. The amide I′ band, centered at 1650 cm^{-1} in solution was shifted to a lower frequency when BSA (Fig. 1 *A*) or lysozyme was adsorbed onto the hydrophobic support (Fig. 1 *C*), which suggests that a significant conformational change occurred during adsorption. The amide I′ band obtained with α-chymotrypsin also became broader in the adsorbed state (Fig. 1 *D*). In contrast, HLL was adsorbed onto the hydrophobic surface without undergoing any significant change in its amide I′ profile.

Secondary structure

Proteins in solution

The relative secondary structure contents of the four proteins are shown in Table 2. Lysozyme, α-chymotrypsin, and HLL contain 13.2%, 9.5%, and 9.3% asparagine and glutamine side chains, respectively, whereas BSA has only 5%. The CON^2H_2 groups of Asn and Gln side chains absorb significantly in the amide I′ region (Chirgadze et al., 1975). As we wanted to compare the fraction of peptide carbonyl in different secondary structures of these proteins in solution

with those of the adsorbed proteins, the Asn and Gln contributions were not removed from the amide I′ band to obtain the absolute contents in secondary structure of the proteins in solution. Furthermore, it is difficult to remove the Asn and Gln contributions by subtracting the amino acid side-chain absorption from the protein amide I′ absorption, as the molar absorptivities of the free amino acids and those of the residues within the polypeptide backbone are probably different (Goormaghtigh et al., 1994).

Previous infrared analyses based on the same spectral decomposition provided a good estimate of the α-helix content of BSA (Servagent-Noinville et al., 2000) and of the β-sheet content of α-chymotrypsin (Baron et al., 1999), based on comparisons with the known x-ray structures of homologous serum albumin (Carter and Ho, 1994) and α-chymotrypsin (Birktoft and Blow, 1972). Our spectral analysis of lysozyme is also in agreement with the relative integrated intensities published by others (Prestrelski et al., 1991).

The three-dimensional structure of HLL shows a single roughly spherical domain containing a central sheet consisting of eight β-strands and five interconnecting α-helixes (Derewenda et al., 1994c). α-Helices account for 26% of the overall peptide carbonyls in the crystalline HLL, whereas 3_{10}-helices involve 7% of the residues (Lawson et al., 1994). It has been suggested that 3_{10}-helix may adsorb at lower wavenumber than α-helices in ^2H_2O solution due to their tighter geometry (Prestrelski et al., 1991) rather than at 1665 cm^{-1}, as previously reported (Krimm and Bandekar, 1986). We assume that the absorption wavenumbers of 3_{10}-helix and α-helix are close enough to form a single component band at $\sim$1650 cm^{-1}. However, our FTIR analysis gives an overall fraction of helices that is 10% greater than the helix content determined by x-ray crystallography (33%). Infrared analysis yielded a satisfactory estimate of the percentage of the peptide carbonyl groups involved in β-like structures (27%), which did not differ from the value of 26% previously found to account for the β-strands and turns on the basis of x-ray crystallographic data (Lawson et al., 1994).

Surface-induced conformational changes for the reference proteins

BSA loses 13% of its helical domains when it becomes adsorbed onto the OTS surface, whereas the bent domains remain unchanged at $\sim$23% (Table 2). The great unfolding of helices involves increases in the number of hydrated and polar domains and is probably accompanied by an increase in the number of self-associated structures. A similar structural change occurs in human serum albumin when it is adsorbed onto a reversed-phase chromatographic support (Boulkanz et al., 1997).

The conformational changes that occurred in lysozyme (Table 2) consisted of the unfolding of helical structures and the formation of either β-strands (band at 1630 cm^{-1}) or extended strands that could be self-associated with external strands of adjacent protein molecules (band at 1610 cm^{-1}) (Table 1). The global structural change in lysozyme caused by adsorption is a small loss of regular secondary structures concerning 4% of the polypeptide backbone.

The main effect of adsorption onto a hydrophobic surface observed in the case of α-chymotrypsin was an unfolding of the β-sheets. The conformational rearrangement increases the peptide carbonyls involved in the most self-associated extended strands at 1618 cm^{-1} and in hydrated domains (band at 1644 cm^{-1}) (Table 2). The changes in the regular secondary structure of α-chymotrypsin involve 10% of the overall backbone.

Surface-induced conformational change for HLL

The global helix content of HLL is not affected by adsorption (Table 2). Covering the OTS support with HLL at a concentration of 0.01 mg/mL causes no major change in the β-like structure of the protein at 10 min compared with that of the protein in solution. The β-strand content (1632 cm^{-1}) reached 28% at 10 min and 32% at 19 h when the layer of adsorbed lipase was complete (Table 2). This slight folding of the β-strands, not exceeding 4% of the backbone, was offset by losses of hydrated domains (1640 cm^{-1}) and self-associated domains (1618 cm^{-1}) (Table 2). This slow conformational rearrangement was more readily observed with incomplete lipase monolayers and was probably due to protein-protein interactions rather than to protein-surface interactions. The slight β-folding occurred more rapidly (within 10 min) when the HLL concentration was higher than 0.01 mg/mL (data not shown). The average conformational states of the adsorbed HLL molecules were similar once the OTS surface was saturated, whatever the bulk concentration. The first molecules of the enzyme adsorbed onto the bare hydrophobic surface had changed their balance between polar and hydrophobic external regions without any drastic changes in their secondary structure. As the monolayer becomes completed by other lipase molecules, the average conformation of the enzymes is more folded.

Tertiary structure

Isotope exchange in proteins in solution

The rate of the $H/^2H$ exchange occurring in the amide CONH bonds of proteins can be measured to distinguish between the fast-exchanging protons of the external amide bonds of the protein and the slower-exchanging protons located in less accessible domains, such as the more hydrophobic secondary structures and the most rigid clusters inside the protein core (Gregory and Lumry, 1985). The $H/^2H$ exchange undergone by each protein in response to exposure to the deuterated buffer is monitored by the amide

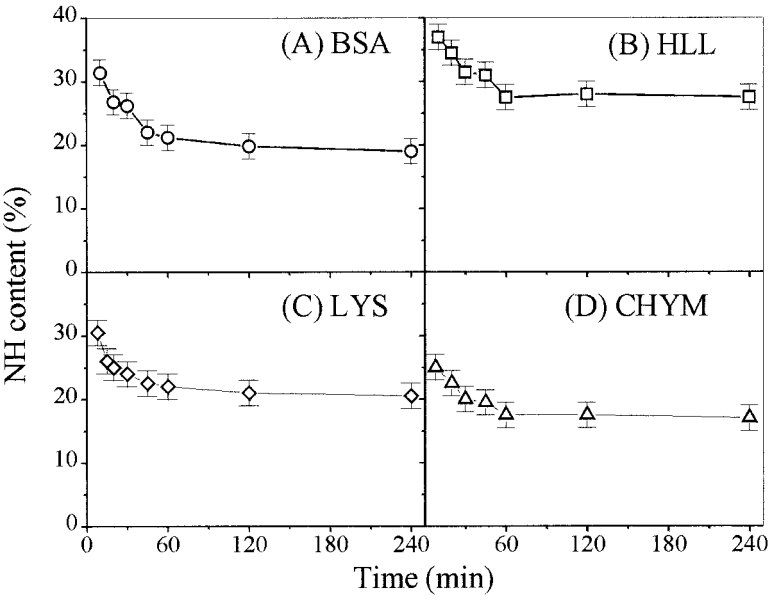

FIGURE 2 Changes in the residual amounts of peptide NH signal with time (in percentage of the overall peptide carbonyls) for BSA (*A*), HLL (*B*), lysozyme (*C*), and α-chymotrypsin (*D*) in deuterated phosphate buffer at p^{2}H 7.5, at 5 mg/mL for HLL, and 4 mg/mL for the three other proteins.

II/amide I′ ratio measurements (Fig. 2). The beginning of the exchange always involved the fully CONH protein and was extremely fast at first (during the first 10 min in contact with ^2H_2O): 70% of the peptide CONH in BSA and lysozyme had become CON^{2}H at 10 min, whereas 75% of the amide protons in α-chymotrypsin had been exchanged. NMR spectroscopy and neutron diffraction revealed that the exchange behavior was similar to that of lysozyme (Bentley et al., 1983). HLL, in contrast, only exchanged 63% of its peptide CONH in CON^{2}H. The lipase backbone is in average less accessible to the aqueous medium. The second step in the H/^{2}H exchange is much slower and takes around 2 h to reach equilibrium (Fig. 2). The content of remaining undeuterated peptides was 17% in the case of α-chymotrypsin, 19% in that of lysozyme, and 20% in that of BSA, whereas the amide CONH level still amounted to 27% in HLL.

Isotope exchange for adsorbed reference proteins

Fig. 3 shows the H/^{2}H exchange rate and the protein adsorption density (Γ) recorded over time with each protein at 0.01 mg/mL. Both BSA and lysozyme were maximally adsorbed quite fast, within 30 min, whereas the peptide NH content decreased drastically to 5%. The greater solvation of the peptide carbonyls due to the diffusion of ^2H_2O molecules into the protein core is directly correlated with the conformational changes in these two α-helical proteins that occurred within 10 min (Table 2).

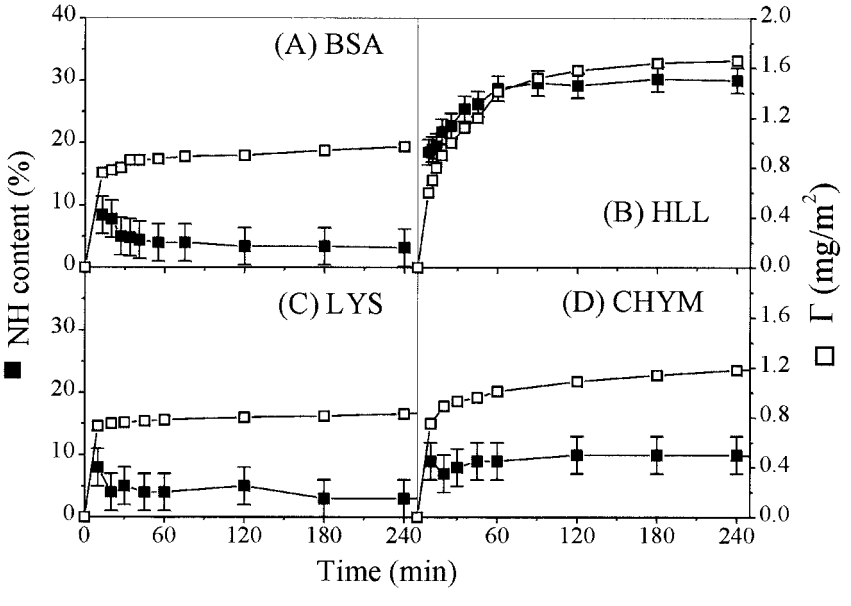

FIGURE 3 Changes in the residual amounts of peptide NH signal (in percentage of the overall peptide carbonyls) (-■-) and protein surface density Γ (-□-) with time for BSA (*A*), HLL (*B*), lysozyme (*C*), and α-chymotrypsin (*D*) (bulk concentration of 0.01 mg/mL) adsorbed onto the hydrophobic surface at p^{2}H 7.5.

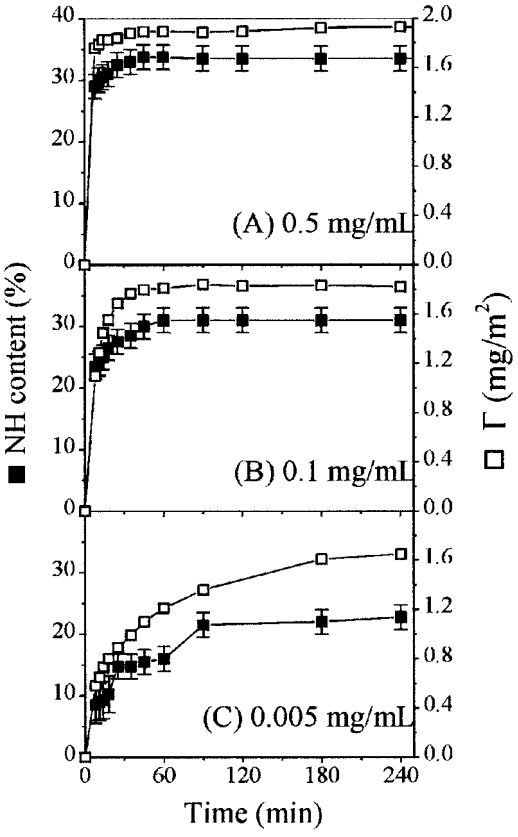

FIGURE 4 Changes in the residual amounts of peptide NH signal (in percentage of the overall peptide carbonyls) (-■-) and of the surface density Γ (-□-) with time for HLL adsorbed onto the hydrophobic surface at p^{2}H 7.5, at bulk concentrations of 0.5 mg/mL (*A*), 0.1 mg/mL (*B*), and 0.005 mg/mL (*C*).

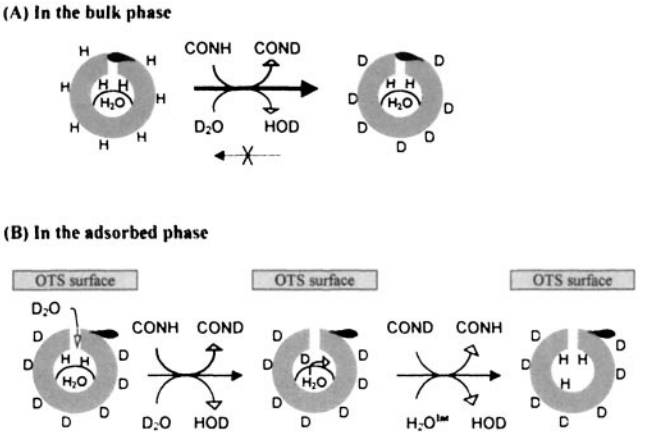

FIGURE 5 CONH/CON^{2}H exchange for HLL in the bulk (*A*) and for the adsorption of lipase at an interface (*B*). The lipase molecules are represented by a dotted ring (*gray*) with a water-filled cavity (*white*) together with the lid (*black spot*) in its closed (in the bulk) or open (at the interface) conformations. For the sake of simplicity, H stands for hydrogen and D for deuterium atoms. The direction of the bold arrows indicates the major flux of the CONH/COND exchange, the reverse exchange is too slow because of the enormous concentration of D_2O molecules in the bulk (*A*). The water shuttle model is depicted in two steps: the CONH/COND exchange by neighboring D_2O molecules followed by the reverse exchange reaction with the internal water molecules (*B*).

α-Chymotrypsin has a higher affinity for the hydrophobic surface than BSA and lysozyme (Fig. 3 *D*). Although 10% of the amide protons in the adsorbed α-chymotrypsin molecules are never exchanged. This large H/^{2}H exchange is also associated with the more unfolded state of the α-chymotrypsin in contact with the hydrophobic surface. The penetration of ^2H_2O molecules into the adsorbed molecules of BSA and α-chymotrypsin was correlated with the increase in the size of the hydrated domains (Table 2).

Isotope exchange in adsorbed HLL

Figs. 3 *B* and 4 illustrate the isotope exchange during the adsorption of HLL onto OTS surface at various HLL bulk concentrations. The value of the residual peptide NH content after 8 min of adsorption varied with the HLL bulk concentration (Fig. 4). The higher the lipase concentration, the higher the residual NH content became. These data indicated that the exchange process is a two-step process.

In the first step, occurring during the first 8 min of adsorption, an exchange of most of the CONH for CON^{2}H peptide bonds leads to a rapid decrease in the NH content of HLL, much like that observed with the other proteins tested (Fig. 3). As there were no significant changes in the secondary structure of HLL at the early stage of the adsorption, in sharp contrast with what occurred with the other three proteins tested (Table 2), a change in tertiary structure had occurred. A relatively limited molecular rearrangement of the HLL, such as the lid opening, could explain the accessibility of new CONH groups to the ^2H_2O solvent (see Fig. 5B).

The second step (after 8 min of adsorption) involves a slow increase in the peptide NH content of HLL (Figs. 3 *B* and 4), reaching a quasi equilibrium value after ~60 min. The plateau value observed was also due to the HLL bulk concentration. The increase in the NH content is specifically correlated with HLL adsorption, because it was not observed with any of the other three proteins tested (see Fig. 3). In a subsequent pre-incubation experiment, we further examined the effects of the exposure time (4 h) of HLL to the ^2H_2O molecules before the beginning of the adsorption onto the OTS surface. In the latter experiment, the interfacial isotope exchange kinetics were found to be similar to the standard pattern measured without any pre-incubation (data not shown). The overall increase in CONH during HLL adsorption could occur if the first adsorbed HLL molecules were in the open form and the subsequent adsorbed ones were also immobilized but less accessible to the solvent due to protein-protein interactions.

This specific increase in the peptide NH content in HLL may also be due to the reverse H/^{2}H exchange because of local protons trapped in hydrophobic domains of the immo-

TABLE 3 Experimental adsorption densities and properties of the proteins

	BSA	HLL	Lysozyme	α-Chymotrypsin
Molecular weight (g/mol)	65,000	22,000	14,500	25,000
Dimension (Å)	$30 \times 80 \times 80$*	$35 \times 45 \times 50$†	$45 \times 30 \times 30$‡	$50 \times 60 \times 60$§
Monolayer (mg/m^2)¶	3.9–4.6	2.3–3–3.3	1.75–2.7	1.15–1.4
Experimental Γ_{limit} (mg/m^2)	1.1	1.9	0.85	1.2

*Carter and Ho, 1994.
†Lawson et al., 1994.
‡Kurinov et al., 1995.
§Biktoft and Blow, 1972.
¶Adsorption density calculated as closed-packed rods following side-on and end-on orientations.

bilized proteins. The protons could be from interfacial HO^{2}H molecules produced during the first step. However, interfacial HO^{2}H molecules are produced during the CONH/CON^{2}H exchange for the four immobilized proteins but the reverse H/^{2}H exchange is only observed for HLL. The source of protons in the lipase is more likely to be internal water molecules rather than transitory HO^{2}H molecules. There are free water molecules near the internal cavity of HLL and these could be released during the adsorption onto the interface, concomitantly with the lid opening. These local reservoirs of water molecules might exchange their protons with the CON^{2}H bonds of adsorbed HLL (see Fig. 5 *B*). This new molecular mechanism might be called an interfacial water shuttle system. However, assuming all the adsorbed HLL molecules to be in the open conformation, a 12% increase in the NH content (from 8 to 60 min, in Fig. 3 *B*) can be taken to correspond to the exchange of ~32 hydrogen atoms (see Materials and Methods). If one assumes that only one H atom per water molecule is exchangeable, then the 32 water molecules delivered and released by HLL at the interface are enough to account for the above increase in the peptide NH content.

In the previously published three-dimensional structure of *Rhizomucor miehei* lipase (RmL), 12 water molecules with a distinct internal character were identified in addition to the typical 218-ordered water molecules (Derewenda et al., 1992b). In addition to these water features, the authors identified a deep depression, filled with 18 water molecules, adjacent to the lid, which provided the latter with an alternative space when its conformation changes upon the opening of the RmL. Interestingly, most of the above mentioned water molecules identified in the closed form of RmL were expelled while the lid was opening (Derewenda et al., 1992a). It is worth noticing that the three-dimensional structure of HLL is highly homologous to that of RmL and that it also contains an internal ordered water pool (Derewenda et al., 1994b).

Adsorption kinetics

The rates at which HLL (Fig. 3 *B*) and the three other proteins (Fig. 3, *A*, *C*, and *D*) were adsorbed onto the hydrophobic support were measured at a bulk concentration of 0.01 mg/mL. The surface densities (Γ) of the adsorbed proteins increased with time and each reached a plateau. The average cross-sectional areas of the protein adsorbed were calculated, assuming that the plateau reached the Γ limit value at the end of adsorption (Table 3).

The calculated cross-sectional area of BSA adsorbed onto OTS was 97 nm^2/molecule (see Table 3). Cross-sectional areas of 99 and 100 nm^2/molecule have been published for BSA on hydrophobic supports at pH 7.0 (Jeon et al., 1994) in good agreement with our results. The unfolding of the adsorbed BSA due to the large increase in ^2H_2O diffusion within the protein core (see surface-induced conformational changes for reference proteins) could explain the fourfold increase in the cross-sectional area at the liquid-solid interface. The same conclusion can be drawn in the case of the lysozyme. However, adsorption of lysozyme at a concentration of 0.01 mg/mL can result in incomplete monolayers (Arai and Norde, 1990). In the case of α-chymotrypsin, circular dichroism spectroscopy has shown the formation of multilayers onto hydrophobic supports (Zoungrana et al., 1997).

For HLL, a plateau value of 1.9 mg/m^2, which corresponds to a cross-sectional area of 27 nm^2/molecule, was rapidly reached at a bulk concentration higher than 0.1 mg/mL (Fig. 4 *A*). The size of the HLL molecule, estimated from the x-ray three-dimensional structure, is $35 \times 45 \times 50$ Å^3 (Derewenda et al., 1994a). Hence, the theoretical values obtained in the case of a densely packed monolayer of HLL are either 3.3 or 3.0 or 2.3 mg/m^2, depending on the protein orientation, corresponding to 16, 18, or 23 nm^2 per HLL molecule, respectively. The slightly higher experimental cross-sectional area (27 nm^2), as compared with the above theoretical values, indicates that the HLL molecules adsorbed on OTS surface do not undergo any significant change in their secondary structure. A loosely packed monolayer of HLL on a polystyrene support has been described with a Γ of 1.5 mg/m^2, corresponding to a molecular area of 34 nm^2 (Martinelle et al., 1995). The more hydrophobic character of the OTS than polystyrene leads to the formation of a more closely packed monolayer of HLL on the OTS-treated surface.

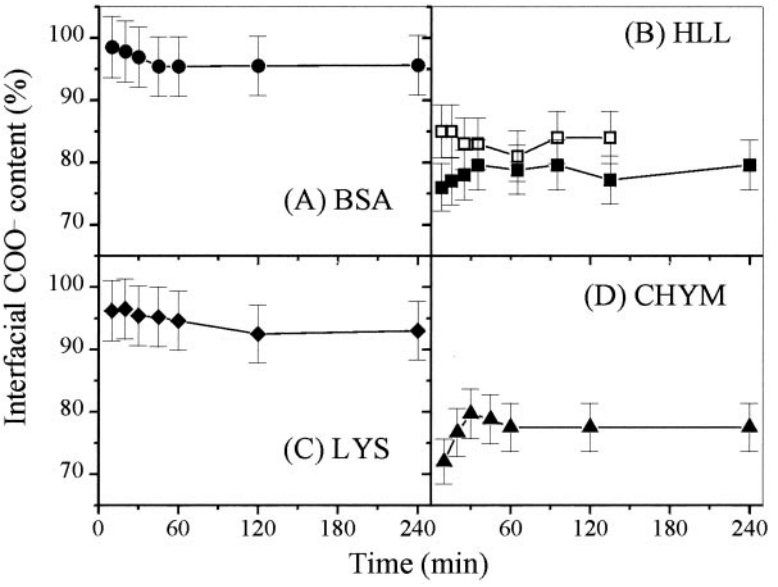

FIGURE 6 Changes in the amounts of COO^- (%) in proteins adsorbed onto the hydrophobic surface at p^2H 7.5. (*A*) BSA at a bulk concentration of 0.01 mg/mL (−●−); (*B*) HLL at bulk concentrations of 0.01 mg/mL (−■−) and 0.5 mg/mL (−□−); (*C*) lysozyme at a bulk concentration of 0.01 mg/mL (−◆−); and (*D*) α-chymotrypsin at a bulk concentration of 0.01 mg/mL (−▲−).

Orientation of HLL at the interface

Fig. 6 shows the changes in the interfacial COO^- contents (%) of HLL and the other proteins adsorbed onto the hydrophobic surface with time. Based on the well-known pK_a values, it can be assumed that all the Asp and Glu side chains in each of the protein molecules are fully deprotonated in solution at p^2H 7.5.

As expected, the hydrophobic support does not significantly affect the rate of protonation of BSA (Fig. 6 *A*) or lysozyme (Fig. 6 *C*), which was the same as in the bulk solution (100%). BSA and lysozyme are adsorbed onto the hydrophobic surface by rearranging their hydrophobic domains toward the substrate, so that the majority of the ionizable groups continue to be influenced by the solvent, as occurs with the protein in solution.

In contrast, ~20% of the carboxylate functions of α-chymotrypsin were found to remain protonated upon adsorption (Fig. 6 *D*). Based on its three-dimensional structure of α-chymotrypsin (Birktoft and Blow, 1972), it is worth noting that most of the 14 Asp and Glu residues lie at the periphery of the enzyme and that external hydrophobic domains containing some carboxylate functions are uniformly distributed over the external surface of the enzyme. The shift of the apparent pK_a of the carboxylate functions directed toward the hydrophobic OTS surface might explain their protonation. This feature does not imply that any specific interfacial orientation of α-chymotrypsin is required.

The adsorbed HLL molecules contained 15% carboxylic functions on average at a bulk concentration of 0.5 mg/mL and 20% at 0.01 mg/mL (Fig. 6 *B*). This average COOH content corresponds to the protonation of ~4 or 5 Asp and/or Glu side chains (Lawson et al., 1994). We identified five carboxylic side-chain residues (Asp-96, Asp-201, Asp-254, Glu-87, Glu-210) near the large hydrophobic surface of HLL (Fig. 7). One should recall that the opening of the lid, induced by contact with the OTS surface, creates a large hydrophobic area at the HLL surface (Fig. 7 *B*). This contact may be responsible for the shift in the local apparent pK_a of these Asp and/or Glu residues, leading to their protonation. The protonation process is most likely to occur when the adsorbed lipases are in the open conformation.

CONCLUSION

FTIR-ATR spectroscopy is a powerful technique for determining the amount of protein adsorbed at a solid/liquid interface as well as for monitoring conformational changes in the protein backbone in situ. This is illustrated by our results for proteins of different structural stabilities. The adsorption of BSA, lysozyme, and α-chymotrypsin onto the hydrophobic support greatly decreases the interface NH content, corroborating the changes in their secondary structures.

In contrast, the decrease in NH content at the early stage of HLL adsorption occurs without any change in the secondary structures of the lipases. The stability of the secondary structure, together with the changes in the tertiary structure, suggest that HLL adopts an open conformation at the water/hydrophobic interface. The preferential orientation of an exposed hydrophobic and less hydrated region of HLL, probably corresponding to the lid region, might explain why five of the Asp and Glu side chains of the adsorbed HLL are still protonated.

Finally, analyses using the water shuttle model described above indicate that lipases differ specifically from the other proteins studied during their adsorption onto a hydrophobic surface. These differences involve

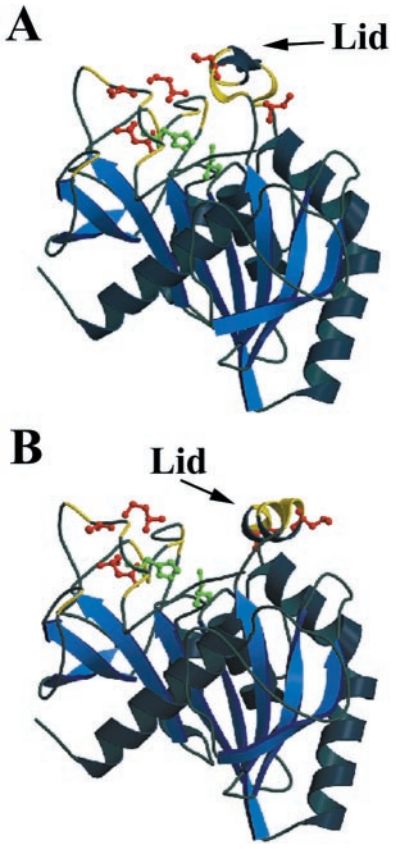

FIGURE 7 Three-dimensional structures of the closed form (*A*) and of the open form (*B*) of HLL. Carboxylic side-chains Asp-96, Asp-201, Asp-254, Glu-87, Glu-210 (in *red*) lie at the periphery of the external hydrophobic region (in *yellow*) The catalytic triad (in *green*) becomes accessible after opening the lid. The rotation of the lid exposed hydrophobic residues of the amphiphilic helix at the external surface of the enzyme.

their lid opening and water shuttling mechanisms. Furthermore, one might speculate that to ensure efficient interface hydrolysis of lipids (which per se are poorly hydrated), lipases have a unique structural feature that leads to the release of water molecules upon the adsorption/opening process. These sequestered water molecules could serve as co-substrates for lipid substrates, so initiating the hydrolysis involving the first carboxylic ester bonds. This triggering mechanism was long ago found to be of prime importance for the subsequent massive enzymatic hydrolysis of lipids; this hydrolysis often characterized kinetically by long lag periods (Wieloch et al., 1982) and structurally by the existence of interfacial water channels (Patton and Carey, 1979).

This research was partly supported by the European Community (contract BIO4-CT97-2365). We are indebted to Dr. Allan Svendsen (Novo-Nordisk, Bagsvaerd, Denmark) for the gift of lipase and for valuable discussions.

REFERENCES

Alberghina, L. 2000. Protein Engineering in Industrial Biotechnology. Harwood Academic Publishers, Australia.

Andrade, J. D., V. Hlady, A.-P. Wei, C.-H. Ho, A. S. Lea, S. I. Jeon, Y. S. Lin, and E. Stroup. 1992. Proteins at interfaces: principles, multivariate aspects, protein resistant surfaces, and direct imaging and manipulation of adsorbed proteins. *Clin. Mater.*11:67–84.

Arai, I., and W. Norde. 1990. The behavior of some model proteins at solid-liquid interfaces: I. Adsorption from single protein solutions. *Colloids Surf. A Physicochem. Eng. Asp.* 51:1–15.

Ball, A., and R. A. L. Jones. 1995. Conformational changes in adsorbed proteins. *Langmuir.* 11:3542–3548.

Baron, M.-H., M. Revault, S. Servagent-Noinville, J. Abadie, and H. Quiquampoix. 1999. Chymotrypsin adsorption on montmorillonite, enzymatic activity and kinetic FTIR structural analysis. *J. Colloid Interface Sci.* 214:319–332.

Bentley, G. A., M. Delepierre, C. M. Dobson, R. E. Wedin, S. A. Mason, and F. M. Poulsen. 1983. Exchange of individual hydrogens for a protein in a crystal and in solution. *J. Mol. Biol.* 170:243–247.

Birktoft, J. J., and D. M. Blow. 1972. Structure of crystalline-chymotrypsin: V. The atomic structure of tosyl-chymotrypsin at 2 A resolution. *J. Mol. Biol.* 68:187–240.

Bornscheuerand, U. T., and R. J. Kazlauskas. 1999. Hydrolases in Organic Synthesis: Regio- and Stereoselective Biotransformations. Wiley-VCH, Weinheim, New York.

Boulkanz, L., C. Vidal-Madjar, N. Balcar, and M.-H. Baron. 1997. Adsorption mechanism of human serum albumin on a reversed-phase support by kinetic, chromatographic, and FTIR methods. *J. Colloid Interface Sci.* 188:58–67.

Brady, L., A. M. Brzozowski, Z. S. Derewenda, E. Dodson, G. Dodson, S. Tolley, J. P. Turkenburg, L. Christiansen, B. Huge-Jensen, L. Norskov, L. Thim, and U. Menge. 1990. A serine protease triad forms the catalytic centre of a triacylglycerol lipase. *Nature.* 343:767–770.

Brzozowski, A. M., U. Derewenda, Z. S. Derewenda, G. G. Dodson, D. M. Lawson, J. P. Turkenburg, F. Bjorkling, B. Huge-Jensen, S. A. Patkar, and L. Thim. 1991. A model for interfacial activation in lipases from the structure of a fungal lipase-inhibitor complex. *Nature.* 351:491–494.

Byler, D. M., and H. Susi. 1986. Examination of the secondary structure of proteins by deconvolved FTIR spectra. *Biopolymers.* 25:469–487.

Carter, D. C., and J. X. Ho. 1994. Structure of serum albumin. *Adv. Protein Chem.* 45:155–203.

Chirgadze, Y. N., O. V. Fedorov, and N. P. Trushina. 1975. Estimation of amino acid residue side-chain absorption in the infrared spectra of protein solutions in heavy water. *Biopolymers.* 14:679–694.

Chittur, K. K. 1998. FTIR/ATR for protein adsorption to biomaterial surfaces. *Biomaterials.* 19:357–369.

de Jongh, H. H., E. Goormaghtigh, and J. M. Ruysschaert. 1996. The different molar absorptivities of the secondary structure types in the amide I region: an attenuated total reflection infrared study on globular proteins. *Anal. Biochem.* 242:95–103.

Derewenda, U., A. M. Brzozowski, D. M. Lawson, and Z. S. Derewenda. 1992a. Catalysis at the interface: the anatomy of a conformational change in a triglyceride lipase. *Biochemistry.* 31:1532–1541.

Derewenda, U., L. Swenson, R. Green, Y. Wei, G. G. Dodson, S. Yamaguchi, M. J. Haas, and Z. S. Derewenda. 1994a. An unusual buried polar cluster in a family of fungal lipases. *Nat. Struct. Biol.* 1:36–47.

Derewenda, U., L. Swenson, R. Green, Y. Wei, S. Yamaguchi, R. Joerger, M. J. Haas, and Z. S. Derewenda. 1994b. Current progress in crystallographic studies of new lipases from filamentous fungi. *Protein Eng.* 7:551–557.

Derewenda, U., L. Swenson, Y. Wei, R. Green, P. M. Kobos, R. Joerger, M. J. Haas, and Z. S. Derewenda. 1994c. Conformational lability of lipases observed in the absence of an oil-water interface: crystallographic studies of enzymes from the fungi *Humicola lanuginosa* and *Rhizopus delemar*. *J. Lipid Res.* 35:524–534.

Derewenda, Z. S., U. Derewenda, and G. G. Dodson. 1992b. The crystal and molecular structure of the *Rhizomucor miehei* triacylglyceride lipase at 1.9 A resolution. *J. Mol. Biol.* 227:818–839.

Desnuelle, P., L. Sarda, and G. Ailhaud. 1960. Inhibition de la lipase pancréatique par le diéthyl-*p*-nitrophényl phosphate en émulsion. *Biochim. Biophys. Acta.* 37:570–571.

Duinhoven, S., R. Poort, G. V. d. Voet, W. G. M. Agterof, W. Norde, and J. Lyklema. 1995. Driving forces for enzyme adsorption at solid-liquid interfaces. *J. Colloid Interface Sci.* 170:351–357.

Ferrato, F., F. Carrière, L. Sarda, and R. Verger. 1997. A critical re-evaluation of the phenomenon of "interfacial activation." *In* Methods Enzymol. E. Dennis and B. Rubin, editors. Academic Press, New York. 327–347.

Fu, F.-N., M. P. Fuller, and B. R. Singh. 1993. Use of Fourier transform infrared/attenuated total reflectance spectroscopy for the study of surface adsorption of proteins. *Appl. Spectrosc.* 47:98–102.

Goormaghtigh, E., V. Cabiaux, and J. M. Ruysschaert. 1990. Secondary structure and dosage of soluble and membrane protiens by ATR FTIR spectroscopy on hydrated films. *Eur. J. Biochem.* 193:409–420.

Goormaghtigh, E., V. Cabiaux, and J. M. Ruysschaert. 1994. Determination of soluble and membrane protein structure by Fourier transform infrared spectrosocpy I: assignments and model compounds. *In* Subcellular Biochemistry. H. J. Hiderson and G. B. Ralston, editors. Plenum Press, New York. 329–362.

Gregory, R. B., and R. Lumry. 1985. Hydrogen-exchange evidence for distinct structural classes in globular proteins. *Biopolymers.* 24:301–326.

Grochulski, P., Y. Li, J. D. Schrag, F. Bouthillier, P. Smith, D. Harrison, B. Rubin, and M. Cygler. 1993. Insights into interfacial activation from an open structure of Candida rugosa lipase. *J. Biol. Chem.* 268: 12843–12847.

Harrick, N. J. 1967. Internal Reflection Spectroscopy. Interscience, New York.

Haynes, C. A., and W. Norde. 1995. Structures and stabilities of adsorbed proteins. *J. Colloid Interface Sci.* 169:313–328.

Imoto, T., L. N. Johnson, A. C. T. North, D. C. Phillips, and J. A. Rupley. 1972. The Enzyme. P. D. Boyer, editor. Academic Press, New York. 665.

Jeon, J. S., S. Raghavan, and R. P. Sperline. 1994. Quantitative analysis of albumin adsorption onto uncoated and poly(ether)urethane-coated ZnSe surfaces using the attenuated total reflection FTIR technique. *Colloids Surf. A Physicochem. Eng. Asp.* 92:255–265.

Kondo, A., F. Murakami, and K. Higashitani. 1992. Circular dichroism studies on conformational changes in protein molecules upon adsorption on ultrafine polystyrene particles. *Biotechnol. Bioeng.* 40:889–894.

Krimm, S., and J. Bandekar. 1986. Vibrational spectroscopy and conformation of peptides, polypeptides, and proteins. *Adv. Protein Chem.* 38:181–364.

Lawson, D. M., A. M. Brzozowski, S. Rety, C. Verma, and G. G. Dodson. 1994. Probing the nature of substrate binding in *Humicola lanuginosa* lipase through x-ray crystallography and intuitive modelling. *Protein Eng.* 7:543–550.

Malmsten, M. 1998. Formation of adsorbed protein layers. *J. Colloid Interface Sci.* 207:186–199.

Martinelle, M., M. Holmquist, and K. Hult. 1995. On the interfacial activation of *Candida antarctica* lipase A and B as compared with *Humicola lanuginosa* lipase. *Biochim. Biophys. Acta.* 1258:272–276.

Momsen, W. E., and H. L. Brockman. 1997. Recovery of monomolecular films in studies of lipolysis. *Methods Enzymol.* 286:292–305.

Netzer, L., and J. Sagiv. 1983. *J. Am. Chem. Soc.* 105:674–676.

Norde, W. 2000. Proteins at solid surfaces. *In* Physical Chemistry of Biological Interfaces. A. Baszkin and W. Norde, editors. Marcel Dekker, New York. 115–136.

Oberg, H. A., and A. L. Fink. 1998. A new ATR-FTIR spectroscopy method for the study of proteins in solution. *Anal. Biochem.* 256:92–106.

Ollis, D. L., E. Cheah, M. Cygler, B. Dijkstra, F. Frolow, S. M. Franken, M. Harel, S. J. Remington, I. Silman, J. Schrag, J. L. Sussman, K. H. G. Verschueren, and A. Goldman. 1992. The α/β hydrolase fold. *Protein Eng.* 5:197–211.

Pantazaki, A., M.-H. Baron, M. Revault, and C. Vidal-Madjar. 1998. Characterization of human serum albumin adsorbed on a porous anion-exchange support. *J. Colloid Interface Sci.* 207:324–331.

Patton, J. S., and M. C. Carey. 1979. Watching fat digestion. *Science.* 204:145–148.

Peters, G. H., A. Svendsen, H. Langberg, J. Vind, S. A. Patkar, S. Toxavaerd, and P. K. J. Kinnunen. 1998. Active serine involved in the stabilization of the active site loop in the *Humicola lanuginosa* lipase. *Biochemistry.* 37:12375–12383.

Prestrelski, S. J., D. M. Byler, and M. P. Thompson. 1991. Infrared spectroscopic discrimination between α- and 3_{10}-helices in globular proteins. *Int. J. Peptide Protein Res.* 37:508–512.

Quiquampoix, H., and R. G. Ratcliffe. 1992. A ^{13}P NMR study of the adsorption of BSA on Montmorillonite using phosphate and the paramagnetic cation Mn^{2+}: modification of conformation with pH. *J. Colloid Interface Sci.* 148:343–352.

Ransac, S., M. Ivanova, R. Verger, and I. Panaiotov. 1997. Monolayer techniques for studying lipase kinetics. *Methods Enzymol.* 286:263–291.

Roussel, A., S. Canaan, M. P. Egloff, M. Rivière, L. Dupuis, R. Verger, and C. Cambillau. 1999. Crystal structure of human gastric lipase and model of lysosomal acid lipase, two lipolytic enzymes of medical interest. *J. Biol. Chem.* 274:16995–17002.

Sarda, L., and P. Desnuelle. 1958. Action de la lipase pancréatique sur les esters en émulsion. *Biochim. Biophys. Acta.* 30:513–521.

Schmid, R. D., and R. Verger. 1998. Lipases: interfacial enzymes with attractive applications. *Angew. Chem. Int. Ed.* 37:1608–1633.

Servagent-Noinville, S., M. Revault, H. Quiquampoix, and M.-H. Baron. 2000. Conformational changes of BSA induced by adsorption on different clay surfaces: FTIR analysis. *J. Colloid Interface Sci.* 221:273–283.

Sperline, R. P., S. Muralidharan, and H. Freiser. 1987. In situ determination of species adsorbed at a solid-liquid interface by quantitative infrared attenuated total reflectance spectrophotometry. *Langmuir.* 3:198–202.

Surewicz, W. K., and H. H. Mantsch. 1988. New insight into protein secondary structure from resolution-enhanced infrared spectra. *Biochim. Biophys. Acta.* 952:115–130.

Swedberg, S. A., J. J. Pesek, and A. L. Fink. 1990. Attenuated total reflectance Fourier transform infrared analysis of an acyl-enzyme intermediate of alpha-chymotrypsin. *Anal Biochem.* 186:153–158.

Tilbeurgh, H. v., M.-P. Egloff, C. Martinez, N. Rugani, R. Verger, and C. Cambillau. 1993. Interfacial activation of the lipase-procolipase complex by mixed micelles revealed by x-ray crystallography. *Nature.* 362:814–820.

Wannerberger, K., and T. Arnebrant. 1996. Adsorption of lipase to silica and methylated silica surfaces. *J. Colloid Interface Sci.* 177:316–324.

Wantyghem, J., M.-H. Baron, M. Picquart, and F. Lavialle. 1990. Conformational changes of *Robinia pseudoacacia* lectin related to modifications of the environment: FTIR investigation. *Biochemistry.* 29: 6600–6609.

Wasserman, S. R., G. M. Whitesides, I. M. Tidswell, B. M. Ocko, P. S. Pershan, and J. D. Axe. 1989. The structure of self-assembled monolayers of alkylsiloxanes on silicon: a comparison of results from ellipsometry and low-angle X-ray reflectivity. *J. Am. Chem. Soc.* 111: 5852–5861.

Wieloch, T., B. Borgstrom, G. Pieroni, F. Pattus, and R. Verger. 1982. Product activation of pancreatic lipase: lipolytic enzymes as probes for lipid/water interfaces. *J. Biol. Chem.* 257:11523–11528.

Winkler, F. K., A. d'Arcy, and W. Hunziker. 1990. Structure of human pancreatic lipase. *Nature.* 343:771–774.

Zoungrana, T., G. H. Findenegg, and W. Norde. 1997. Structure, stability and activity of adsorbed enzymes. *J. Colloid Interface Sci.* 190: 437–448.